



## Effect of high-frequency electromagnetic fields on trophoblastic connexins

Franco Cervellati<sup>a</sup>, Guido Franceschetti<sup>a</sup>, Laura Lunghi<sup>a</sup>, Silvia Franzellitti<sup>b</sup>, Paola Valbonesi<sup>b</sup>, Elena Fabbri<sup>b</sup>, Carla Biondi<sup>a,\*</sup>, Fortunato Vesce<sup>c</sup>

<sup>a</sup> Department of Biology and Evolution, Section of General Physiology, University of Ferrara, via L. Borsari 46, 44100 Ferrara, Italy

<sup>b</sup> Interdepartmental Centre for Environmental Science Research, University of Bologna, Ravenna, Italy

<sup>c</sup> Department of Biomedical Sciences and Advanced Therapy, Section of Obstetrics and Gynaecology, University of Ferrara, Ferrara, Italy

### ARTICLE INFO

#### Article history:

Received 17 November 2008

Received in revised form 2 March 2009

Accepted 27 March 2009

Available online 5 April 2009

#### Keywords:

Cyclic AMP

Connexins

High-frequency electromagnetic fields

Extravillous trophoblasts

Ultrastructure

### ABSTRACT

Connexins (Cx) are membrane proteins able to influence trophoblast functions. Here we investigated the effect of high-frequency electromagnetic fields (HF-EMF) on Cx expression and localization in extravillous trophoblast cell line HTR-8/SVneo. We also analysed cell ultrastructural changes induced by HF-EMF exposure. Samples were exposed to pulse-modulated 1817 MHz sinusoidal waves (GSM-217 Hz; 1 h; SAR of 2 W/kg). Cx mRNA expression was assessed through semi-quantitative RT-PCR, protein expression by Western blotting, protein localization by indirect immunofluorescence, cell ultrastructure using electron microscopy.

HF-EMF exposure significantly and selectively increased Cx40 and Cx43, without altering protein expression. Nevertheless, Cx40 and Cx43 lost their punctuate fluorescence within the cell membrane, becoming diffuse after HF-EMF exposure. Electron microscopy evidenced a sharp decrease in intercellular gap junction-like structures.

This study is the first to indicate that exposure of extravillous trophoblast to GSM-217 Hz signals can modify Cx gene expression, Cx protein localization and cellular ultrastructure.

© 2009 Elsevier Inc. All rights reserved.

### 1. Introduction

In developed countries, the population is constantly exposed to a large number of devices, such as broadcasting systems and mobile telephones, which generate high-frequency electromagnetic fields (HF-EMF) ranging from 30 kHz to 300 GHz. Reports of the effects of these fields on human health are conflicting. For instance, an increased risk of brain cancer has been reported by some authors [1], while, according to others, human health is not adversely affected by exposure to permissible radiofrequency (RF) levels from mobile phones and base stations [2]. As for reproduction, HF-EMFs do not induce a significant increase in reproductive risk in the rat, as assessed by classic postnatal morphological and psychophysiological parameters [3,4]. However, a decrease in the number of mouse offspring, a prevalence of males over females and an increased incidence of stillbirth provoked by irradiation has been reported [5]. Furthermore, ultra-high-frequency electromagnetic field exposure during embryogenesis has been found to induce a genotoxic response in rat haematopoietic tissue [6].

It is conceivable that any obstetric effect of clinical relevance would imply some kind of influence upon gestational tissue. In this

context, it has been demonstrated that HF-EMF exposure results in increased levels of heat-shock protein 70 (HSP 70) in human amnion cells *in vitro* [7], but does not affect the expression of this protein in HTR-8/SVneo cells [8]. However, levels of the inducible *HSP70C* transcript were significantly enhanced after 24 h exposure to GSM-217 Hz signals [9]. In the human first-trimester placenta, extravillous trophoblast cells (EVT) invade uterine spiral arteries to generate a high-capacity, low-resistance utero-placental blood flow for optimal foetal development and growth. Proliferation, migration and invasiveness of EVTs depend on several factors produced by decidua, myometrium and the trophoblast itself [10,11], as well as by gap-junctional intercellular communications (GJIC) [12–15]. These, in turn, are known to influence cell growth, development and differentiation in normal tissues as well as in some pathologic conditions [16].

Gap junctions (GJ) are membrane channels constituted by the association of two hemi-channels, termed connexons, each composed of six connexin subunits. These membrane channels span the intercellular space, thus providing a pathway for the exchange of ions, such as Ca<sup>2+</sup>, and small molecules like cyclic AMP, cyclic GMP (cGMP), and inositol trisphosphate (IP<sub>3</sub>). Cxs represent a family of closely related membrane proteins with different biophysical and regulatory characteristics [17]. They are encoded in humans by a multigene family containing at least 20 members, and their expression is regulated by several hormones and growth factors

\* Corresponding author. Tel.: +39 0532 455482; fax: +39 0532 207143.

E-mail address: [clm@unife.it](mailto:clm@unife.it) (C. Biondi).

[18]. Cx expression is also affected by chemical pollutants [19], ionizing radiations and other environmental stresses [20].

Considering the need to deepen knowledge about the exposure of gestational tissue to magnetic fields, we decided to investigate their effects on HTR-8/SVneo cells. These cells represent a suitable model for the experimental study of early trophoblast function, because they are derived from first-trimester EVT, preserving all of their parental markers and responsiveness towards cell function mediators [21]. Specifically, we evaluated HF-EMF influence on Cx gene and protein expression, as well as Cx localization and ultrastructural cell features.

## 2. Materials and methods

### 2.1. Cell cultures

The HTR-8/SVneo cell line was kindly provided by Doctor CH Graham of Queen's University, Kingston, Ontario, Canada. Cells were grown in RPMI 1640 medium supplemented with 10% foetal bovine serum, 2 mM L-glutamine, 100 U/ml penicillin and 100 µg/ml streptomycin (Invitrogen Paisley, Scotland, UK). Cells were maintained at 37 °C in normal atmosphere containing 5% CO<sub>2</sub>. For the experiments, cells were treated with trypsin, removed from culture flasks, then seeded at a density of 1 × 10<sup>6</sup> cells per 35 mm-diameter Petri dish. After 24–48 h culture, semi-confluent monolayers were exposed to treatments.

### 2.2. Semi-quantitative RT-PCR

Total RNA was extracted using the TRIzol reagent (Invitrogen Paisley, Scotland, UK) from HTR-8/SVneo cell line. Total RNA was dissolved in RNase-free water and subsequently quantified by spectrophotometry. 2 µg of total RNA was reverse-transcribed into complementary DNA (cDNA) using 200 Units of Moloney Murine Leukaemia Virus (M-MLV) Reverse Transcriptase (Invitrogen, Paisley, Scotland, UK), 0.6 µg of random primers and 40 units of RNaseOUT RNase inhibitors (Invitrogen Paisley, Scotland, UK), according to the manufacturer's protocols. Primer pairs used for each gene product were previously reported [14] and are listed in Table 1. As a normalization control for each RT-PCR experiment, primers specific for 18S rRNA were used [22]. For each amplification of Cx and 18S, reactions were performed in a 25 µl final volume containing 1 µl of cDNA template, 1.5 mM of MgCl<sub>2</sub>, 0.2 mM of each dNTP, 0.4 µM of each primer, and 0.5 U of Platinum Taq DNA Polymerase (Invitrogen Paisley, Scotland, UK).

PCR amplifications for all Cx genes were performed under the following conditions: initial denaturation (2 min at 94 °C) followed by different cycles of denaturation (30 s at 94 °C), annealing (1 min at the selected annealing temperature), extension (1 min at 72 °C), and a final extension step (5 min at 72 °C). The applied reaction parameters, which differed between different primer pairs, are reported in Table 1.

To ensure quantification was performed at the midpoint of the linear phase of amplification, preliminary RT-PCRs were carried out for each gene using different dilutions (5-, 10-, 20-, and 40-fold) of each cDNA sample and different PCR cycle numbers.

Equal aliquots of each PCR sample were separated by electrophoresis in a 1.5% agarose gel containing 0.05% ethidium bromide. Quantification of band intensities was performed by the Gel Doc 2000 video image system (Bio-Rad Laboratories, Hercules, USA). 18S rRNA was used as an endogenous control for normalization.

**Table 1**  
Primer sequences and PCR conditions.

Gene	Primer sequence	T <sub>a</sub> °C	Product length (bp)	No. of cycles	Ref.
Cx32	F: 5'-accaattcttcccactctcc-3' R: 5'-ctggtatgtggcatgagca-3'	53	669	32	Nishimura et al. [14]
Cx37	F: 5'-cagcatggagcccgtgtttgt-3' R: 5'-gggacgacttgggggtttttg-3'	58	433	33	Nishimura et al. [14]
Cx40	F: 5'-ccggcccacagagaagaatgt-3' R: 5'-tctgaccttgccttgcctg-3'	60	479	35	Nishimura et al. [14]
Cx43	F: 5'-aaagagatcctgcccacatc-3' R: 5'-cctgggaagaacttagcatcacc-3'	60	370	29	Nishimura et al. [14]
Cx45	F: 5'-caagtccaccgttttatgtg-3' R: 5'-agttcttccatccctgat-3'	60	574	35	Nishimura et al. [14]
18S	F: 5'-ggaccagaggcaagcatttgcc-3' R: 5'-tcaatctcgggtggctgaacg-3'	60	495	30	Spencer et al. [22]

### 2.3. HF-EMF exposure

All experiments consisted of control samples kept at 37 °C and 5% CO<sub>2</sub> in a Forma™ thermostat. Exposed samples were kept in identical Forma™ thermostats which also housed the GSM-exposure system. Cells were exposed for 1 h to a 1.8 GHz sinusoidal wave, whose amplitude was modulated by rectangular pulses with a repetition frequency of 217 Hz, simulating the E net GSM phone emission when the user is speaking [23]. The signal was applied at time-averaged SAR values of 2 W/kg, the safety limit for mobile phone emission according to ICNIRP (International Commission on Non-Ionizing Radiation Protection). The exposure system was developed and built by the Foundation for Research and Information Technologies in Society (IT'IS Foundation, Zurich, Switzerland) following the specifications outlined in Schönborn et al. [24] and extensively described in Valbonesi et al. [8]. The system consisted of two 128.5 mm × 65 mm × 424 mm brass single-mode waveguide resonators operated inside the Forma™ thermostat. Each resonator was equipped with a plastic holder hosting six 35 mm Petri dishes arranged in two stacks. The carrier frequency, modulation, SAR level and the periodically repeated on and off exposure time were controlled by a computer. Cells incubated into the waveguide resonator not selected for irradiation are referred to as sham-exposed samples. The exposure/sham conditions were assigned to the two waveguides by the computer-controlled signal unit. All exposure conditions and monitor data of each single experiment are encrypted in a file, which is decoded by the IT'IS Foundation (Zurich, Switzerland) after data analysis, to ensure blind conditions for the experiment. Inside the exposure system developed and built by the IT'IS Foundation dishes are placed in the H-field maximum of the standing wave inside the waveguide (E polarization). Petri dishes used are of the appropriate size and contain monolayers of cells in appropriate amount and type of medium as requested by the dosimetry developed in the simulation experiments (Schuderer et al., [35]). The simulation results were verified extensively using a near-field scanner DASY3 (SPEAG) equipped with dosimetric field and temperature probes by Schuderer et al. [35]. The results showed the following: 1. The temperature of the monolayer cells is uniformly distributed without localized temperature "hot spots" [35]. 2. The increase in temperature due to the high-frequency EMF is well below 0.1 °C per unit SAR, with a thermal time constant of 280 s for a medium of 3.1 ml in the Petri dish. 3. The temperature difference between sham and exposed cells is less than 0.1 °C. There is no possibility to assess if temperature changes during the experiment; if the imposed conditions are not respected, the computer automatically switches off the instruments and the experiment is stopped. However, direct temperature measurements are routinely performed by us in preliminary experiments using a temperature probe inserted in the medium (T1V3, SPEAG) so to confirm the results of the simulation [35].

### 2.4. Cell viability assay

Cell viability was determined by MTT test, a colorimetric assay based on tetrazolium salt reduction by metabolically active cells as reported by Mosmann [25] with slight modifications since the assay was performed in 12 well culture plates, and optical density was assessed at 570 nm with background correction at 650 nm.

### 2.5. Functional response determination

Cell functionality was tested measuring responsiveness of adenylyl cyclase to receptorial and non-receptorial agents by measuring intracellular cAMP levels. Confluent cells were incubated in serum-free RPMI at 37 °C for 10 min in the presence of 10<sup>-5</sup> M isobutylmethylxanthine (IBMX) (Sigma Chemical Co, St. Louis, MO, USA), a cAMP phosphodiesterase inhibitor, and the test substances (Sigma Chemical Co, St. Louis, MO, USA). The reaction was terminated by removing the medium and adding ice-cold 0.1 N HCl. After centrifugation at 12,500 × g for 10 min, supernatants were

neutralized by 0.5 M trizma base; the cAMP content was determined by the method of Brown et al. [26] and expressed as pmoles/ $10^6$  cells/min.

### 2.6. Western blotting for Cx protein evaluation

After the experimental treatments, cells were washed with ice-cold phosphate-buffered saline solution (PBS), detached by scraping and transferred to Eppendorf tubes. After 10 min centrifugation at  $800 \times g$  at  $4^\circ\text{C}$ , the pellet was resuspended in ice-cold 10 mM Na-phosphate buffer, pH 7.4, containing 1% Nonidet-P40, 0.5% Na deoxycholate, 0.1% SDS, 1  $\mu\text{g}/\text{ml}$  of pepstatin A, E-64, bestatin, leupeptin and aprotinin, 25  $\mu\text{g}/\text{ml}$  of PMSF. After 30 min on ice samples were centrifuged at  $9000 \times g$  at  $4^\circ\text{C}$  for 20 min. The supernatant was diluted 1.5 times with Laemmli buffer [27], boiled for 5 min and kept at  $-20^\circ\text{C}$  until use. Sample proteins were assessed according to Lowry et al. [28] using bovine serum albumin as standard. Western blotting procedures were carried out as we previously reported [29]; briefly, electrophoresis was carried out with a Mini Protean III apparatus (28 mA, 2 h at  $4^\circ\text{C}$ ), and the resolved proteins were transferred onto a nitrocellulose membrane (300 mA, 1 h at  $4^\circ\text{C}$ ). Connexins were assessed by using Cx40 and Cx43 rabbit polyclonal antibodies (Santa Cruz Biotechnology Inc. CA, USA) against connexins of human origin as primary antibodies (1:200) overnight and, after washings, with goat anti-rabbit IgG (1:2000) conjugated with horseradish peroxidase for 1 h (Cell signaling Technology Inc. Beverly, MA, USA). Immunoblots were developed by enhanced chemiluminescence reagent, and a densitometric analysis of the films was performed by Image Master (Amersham-Pharmacia, Milan, Italy) equipped with TotalLab software. Values within each experiment were normalized to the control sample, i.e. unstressed cells kept at  $37^\circ\text{C}$ , and data of connexins were expressed as sham and irradiated forms.

### 2.7. Indirect immunofluorescence staining of Cx

HTR-8/SVneo cells were incubated in serum-free medium for 24 h, then cells ( $1.5 \times 10^6/\text{ml}$ ) were allowed to adhere onto glass coverslips overnight. Adherent cells were prefixed with 1% paraformaldehyde (PFA) for 3 min, washed in phosphate-buffered salt solution (PBS; 0.01 M, pH 7.2) and labelled with different rabbit antibodies raised against the human Cx40 and Cx43 (working dilutions 1:200 in PBS containing 0.05% BSA and 0.1% sodium azide) for 1 h at room temperature (RT) without any cell permeabilization. All antisera specifically recognize the C-terminus of the different human Cxs; in particular, Cx40 antisera were raised against amino acids 231–346 mapping within a C-terminal domain of Cx40 of human origin, Cx43 antisera were raised against amino acids 233–382 mapping at the C-terminus of Cx43 of human origin, respectively. Specificity of antibodies binding was accomplished by blocking with their cognate peptides. Cells were then washed in PBS and incubated with FITC-labelled goat anti-rabbit IgG serum (diluted 1:100 in PBS) for 1 h at RT in the dark (Santa Cruz Biotechnology Inc. CA, USA). Controls included labelling with secondary antibody alone in the absence of primary antibody. Cells were washed in PBS, postfixed with 3% PFA for 3 min, rinsed in PBS, mounted in Vectashield (Vector Labs, Burlingame CA, USA) anti-fading in the dark and observed (excitation wavelength: 488 nm, emission: 520 nm) with a Epi-fluorescence microscope Nikon Eclipse E800 (Nikon Corporation, UK) equipped with a plan apochromat  $100 \times 0.5$ -1.3 oil immersion objective and an mercury lamp source. Amplifier and detector optimizing parameters were maintained constant for all the experiments.

### 2.8. Ultrastructural study

Cells were scraped and collected in 0.1 M cacodylate buffer (pH 7.4), then spun in 1.5 ml tubes at  $2000 \times g$  for 5 min. Pellets were fixed with 2.5% glutaraldehyde in 0.1 M sodium cacodylate buffer for 4 h at  $4^\circ\text{C}$ . They were then washed with 0.1 M cacodylate buffer (pH 7.4) three times and post-fixed in 1% osmium tetroxide and 0.1 M cacodylate buffer at pH 7.4 for 1 h at room temperature. The specimens were dehydrated in graded concentrations of ethanol and embedded in epoxide resin (Agar Scientific, 66A Cambridge Road, Stanstead Essex, CM24 8DA, UK).

Cells were then transferred to latex modules filled with resin and subsequently thermally cured at  $60^\circ\text{C}$  for 48 h.

Semi-thin sections (0.5–1  $\mu\text{m}$  thickness) were cut using an ultra-microtome (Reichard Ultracut S, Austria) stained with toluidine blue, and blocks were selected for thinning. Ultra-thin sections of about 40–60 nm were cut and mounted onto formvar-coated copper grids. These were then double-stained with 1% uranyl acetate and 0.1% lead citrate for 30 min each and examined under a transmission electron microscope, Hitachi H-800 (Tokyo, Japan), at an accelerating voltage of 100 KV.

### 2.9. Statistical analysis

All data were subjected to statistical analysis using PRISM software (version 2.1, Graph Pad Inc.). Data were examined by one-way ANOVA followed by Dunnett's *post hoc* Multiple Comparison test. Specifically, tests were performed to ensure that the sham-exposed samples were not significantly different from one another. When these conditions were met, a second one-way ANOVA was performed on the data from the sham- and HF-EMF-exposed groups. In all cases statistically significant difference was accepted when  $p < 0.05$ .

## 3. Results

### 3.1. Viability of HTR-8/SVneo cells

As revealed by the MTT test, there was no significant difference in cell viability between the negative control (incubator) and the sham-exposed cells. Viability of exposed samples (1 h to GSM-217 Hz signals) was always greater than 98% with respect to sham-exposed samples.

### 3.2. Functional response of HTR-8/SVneo cells

In order to investigate cell functionality, we tested the responsiveness of adenylyl cyclase to receptorial and non-receptorial agents by measuring intracellular cAMP levels. Prostaglandin  $\text{E}_2$  ( $\text{PGE}_2$ ) and epinephrine (EPI) increased cAMP levels in a dose-dependent manner, reaching a plateau at  $10^{-5}$  M. Similarly, forskolin, a direct activator of the catalytic subunit of the enzyme, dose-dependently enhanced intracellular cAMP concentration, reaching maximum response at  $10^{-5}$  M (Fig. 1A), as previously reported [30]. These effects were not modified by 1 h irradiation (Fig. 1B).

### 3.3. Cx mRNA expression in HTR-8/SVneo cells

Under basal conditions, semi-quantitative RT-PCR analysis demonstrated that HTR-8/SVneo cells express detectable levels of the transcripts for Cx32, Cx37, Cx40, Cx43 and Cx45 (Fig. 2).

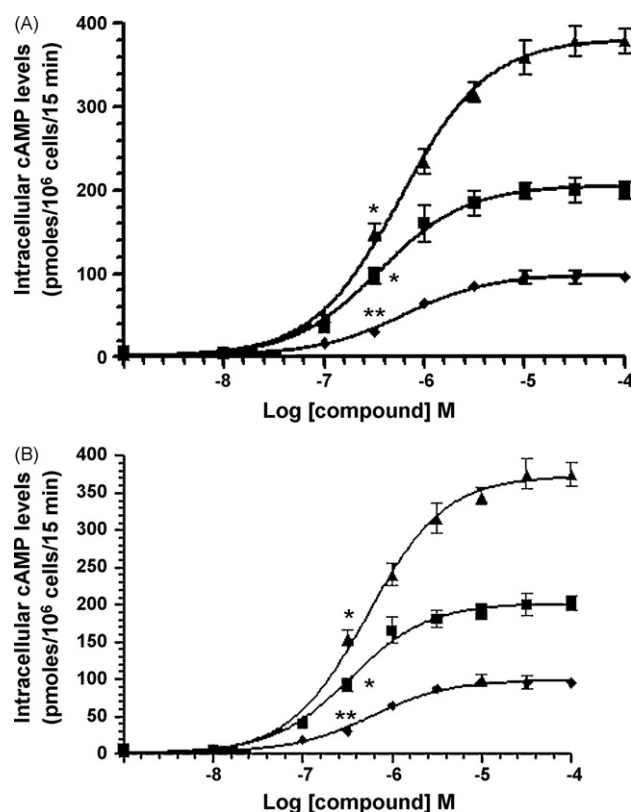


**Fig. 1.** Effect of various concentrations of  $\text{PGE}_2$  (■), epinephrine (◆) and forskolin (▲) on intracellular cAMP levels in HTR-8/SVneo cells. (A) Control cells; (B) cells treated with HF-EMF for 1 h. Data are means  $\pm$  SEM of five experiments, performed in duplicate on different cell cultures. Basal cAMP level was  $6.1 \pm 0.5$  pmoles/ $10^6$  cells/10 min in control cells and  $5.7 \pm 0.4$  pmoles/ $10^6$  cells/10 min in treated samples. Concentration at which the compounds stimulation become statistically significant, \*  $p < 0.01$ , \*\*  $p < 0.05$  (one-way ANOVA followed by Dunnett's *post hoc* Multiple Comparison test).

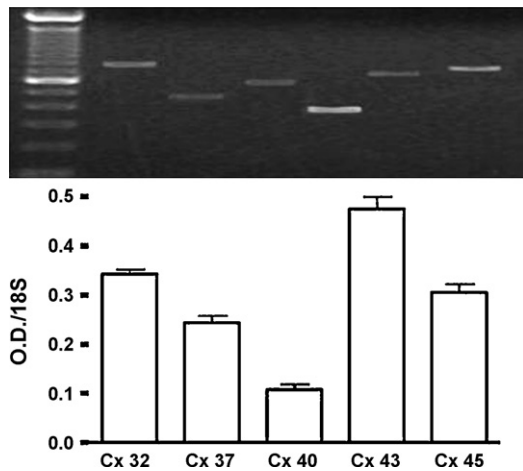


**Fig. 2.** Semi-quantitative analysis of PCR products of different connexin isoforms in HTR-8/SVneo cells.

The panel shows the ratio between optical density (OD) of the Cx mRNA isoforms and 18S mRNA. Data are means  $\pm$  SEM of at least six independent experiments. Representative agarose gel electrophoresis of PCR for Cx isoforms and relative control loading 18S housekeeping gene amplicons is shown in the top of each panel. M: 100 bp ladder DNA marker; lane 1: Cx32; lane 2: Cx37; lane 3: Cx40; lane 4: Cx43; lane 5: Cx45; and lane 6: 18S housekeeping gene.

One-hour exposure to GSM-217 Hz signals did not change expression levels for the Cx32, Cx37 and Cx45 gene products, whereas it significantly increased that for Cx40 (175%;  $p < 0.001$ ) and Cx43 (166%;  $p < 0.001$ ) as compared to sham-exposed cells (Fig. 3).

#### 3.4. Cx protein expression in HTR-8/SVneo cells

The expression of Cx43 and Cx40 proteins was evaluated using specific antibodies (Fig. 4). No significant differences in either Cx43 or Cx40 expression were observed between high-frequency EMF-exposed and sham-exposed samples.

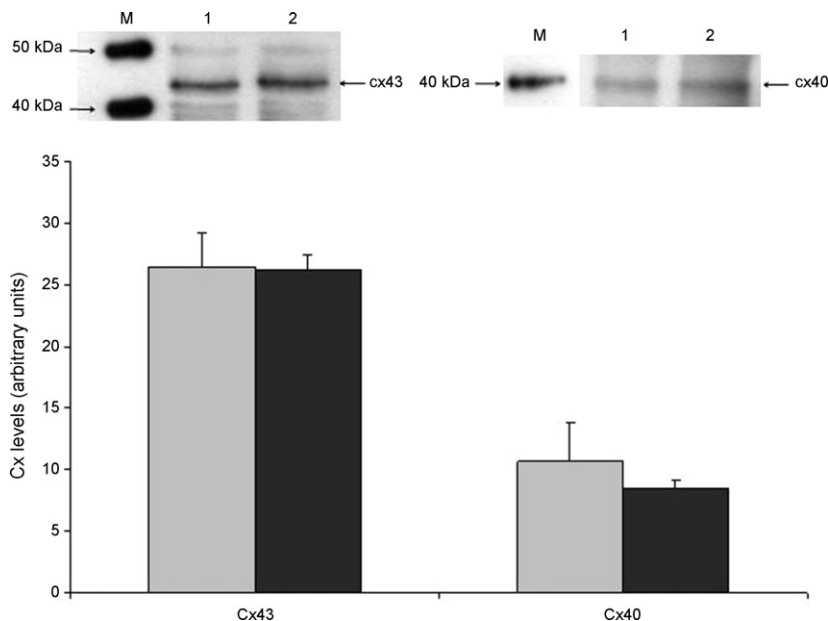


**Fig. 4.** Western blot detection of Cx protein expression in HF-EMF-exposed HTR-8/SVneo cells. Representative immunoblots of Cx43 and Cx40 are shown: M: marker; lane 1: Cx detected in sham-exposed cells; lane 2: Cx detected in HF-EMF-exposed cells. Densitometric analysis shows the levels of Cx43 and Cx40 in sham- (white bar) and HF-EMF-exposed (black bar) cells, expressed as arbitrary units. Results are the means  $\pm$  SEM of five independent experiments, each analysed in triplicate.

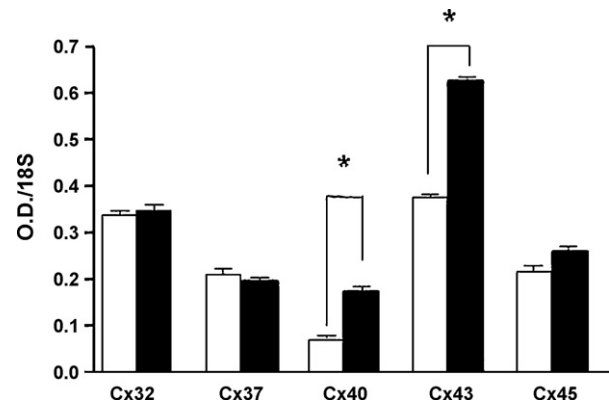


**Fig. 3.** Semi-quantitative analysis of PCR products in HF-EMF-exposed HTR-8/SVneo cells.

The panel shows the ratio between optical density (OD) of Cx mRNA isoform and 18S mRNA in sham- (white bar) and HF-EMF-exposed (black bar) cells. Data are means  $\pm$  SEM of at least five independent experiments. \*  $p < 0.001$  vs relative sham-exposed cells (one-way ANOVA followed by Dunnett's *post hoc* Multiple Comparison test).

#### 3.5. Cx immuno-localization in HTR-8/SVneo cells

In sham-exposed cells we found punctate fluorescence for both Cx40 and Cx43 in plasma membrane clusters (Fig. 5A and C). In HF-EMF irradiated cells, instead, large amount of fluorescence became diffuse in plasma membrane (Fig. 5B and D).

#### 3.6. Ultrastructural features of HTR-8/SVneo cells

Electron microscopy examination of selected areas of HTR-8/SVneo control cells showed that neighbouring cells were in close apposition with each other, forming compact cellular islets and maintaining their epithelial phenotype. The fine structure of cells showed a high nuclear-cytoplasmic ratio and irregularly shaped plasma membranes presenting several pseudopodial protrusions. In the extracellular space close to the cells, some gap junction-like

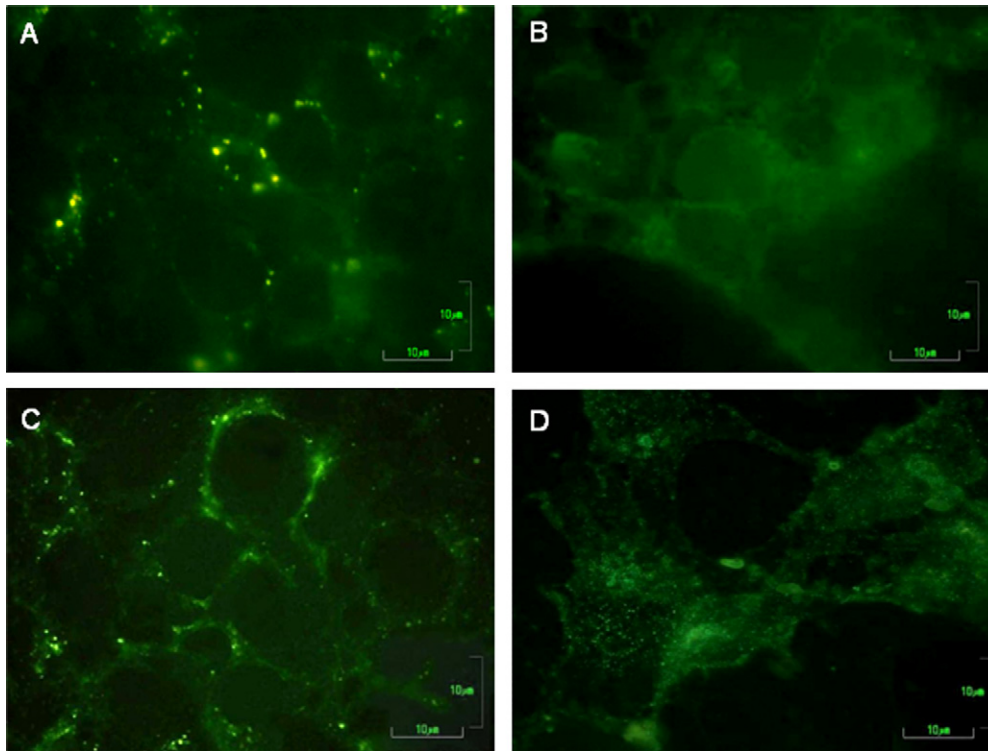


**Fig. 5.** Indirect immunofluorescence staining of Cx in HTR-8/SVneo cells. Sham-exposed cells Cx40 (A); HF-EMF-exposed cells Cx40 (B); Sham-exposed cells Cx43 (C); HF-EMF-exposed cells Cx43 (D). Scale bars = 10  $\mu$ m.

structures, exhibiting considerable electron density, were observed. The cytoplasm of most cells contained single particles and clusters of glycogen and filaments of collagen-like material, as well as many ribosomes displayed on the surface of the rough endoplasmic reticulum (Fig. 6A). Sham-exposed cells did not show ultrastructural morphological changes in comparison with control cells (Fig. 6B). In HF-EMF exposed cells, however, remarkable changes were present. Indeed, retraction of cell surface pseudopods, decrease in cellular adhesion, widening of intercellular spaces, along with cellular flattening and epithelial-like polygonal cell formation, were observed. Gap junction-like structures were only maintained in the internal part of tightly adherent cell islets. Cell surface micromorphology and intercellular junction changes appeared to be closely related to cytoskeletal filament disorganization. A marked cytoplasmic degranulation and vacuolization was manifested as dilatation and fragmentation of the endoplasmic reticulum cisternae. Abnormalities in the mitochondrial structure consisted of matrix swelling and vacuolization accompanied by cristae disruption (Fig. 6C).

#### 4. Discussion

It is well known that successful pregnancy relies upon trophoblast cell proliferation, migration and invasiveness. Pathologic conditions of pregnancy, such as choriocarcinoma and pre-eclampsia, can derive from subversion of above-mentioned processes. Social behaviour of trophoblast cells is regulated, among other factors, by gap-junctional intercellular communication [13,14]. This, in turn, depends on the expression of connexins, which can be affected by several types of environmental stresses [19,20]. With regard to human trophoblast, it has been shown that Cx40 and Cx45 are typically expressed in the extravillous cell columns. Cx40 disappears when the proliferative cell phenotype changes to invasive, to be later re-expressed in the trophoblastic

cell aggregates within the decidua [13,14,31]. At the level of placental bed aggregates also Cx43 and Cx32 are expressed [12,32]. Finally Cx37, which is typically present in the endothelium of villous arterioles, is also found in extravillous cells, and weakly expressed at the cytotrophoblast level, as well as between the cytotrophoblast and syncytial layer [29]. In general, it appears that Cx40 participates in cell proliferation while Cx43 is involved in the processes of cell fusion, such as formation of multinuclear aggregates and syncytialization [33]. *In vitro* studies on isolated cells have shown that Cx43 is abundant in the normal EVT HTR-8, while it is reduced in the long-lived (RSVT-2) and undetectable in the immortalized cell line [34].

In our study, at first we tested the expression of connexin mRNA in first-trimester human chorionic villi at the 11th gestational week, confirming the presence of Cx32, Cx37, Cx40, and Cx43, but not Cx45 mRNA (data not shown). This result is in agreement with literature data showing that expression of Cx45 disappears after the 9th week, due to sharp oxygen increase at the level of placental lakes [14]. Chorionic villi were obtained from consenting patients undergoing villous biopsy for foetal chromosomal analysis, in order to compare Cx expression with that of an immortalized cell line such as HTR-8/SVneo. In fact, HTR-8/SVneo were chosen as the cell model for studying the possible effects of HF-EMF. Chorionic villi were not suitable for our study protocol on HF-EMF effects, due to the strict conditions required to fulfil the dosimetric parameters of the instruments, in particular a cell monostrate [24,35]. HTR-8/SVneo cells were then chosen as an *in vitro* model, in order to analyse the possible effects of HF-EMF on first trimester trophoblast connexin expression and localization. The reason why we addressed our attention to this topic is because pregnant women are commonly exposed to a large number of devices generating high-frequency electromagnetic fields. It is therefore of utmost importance to assess any possible influence exerted by this sort of energy upon gestational tissue.

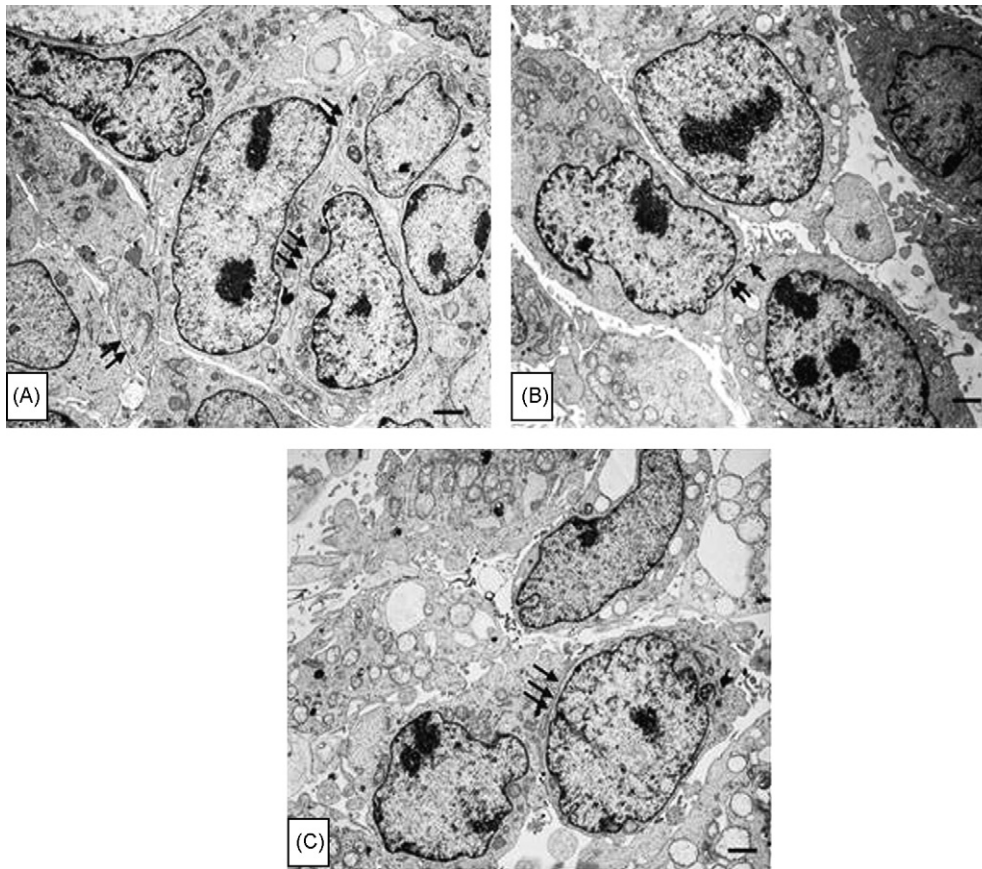


**Fig. 6.** Electron microscopy of HTR-8/SVneo cells under different experimental conditions. Confluent culture cells in serum-supplemented medium (A). Cells tightly contacting each other with gap junction-like structures are represented by arrows. Mitochondria, endoplasmic reticulum, nuclear membranes and euchromatic nucleus with marginal heterochromatin show normal morphological features; serum-free culture medium (sham-exposed cells): the cells maintain substantially unchanged their morphology (B); HF-EMF-exposed cells showing mitochondrial vacuolization and sharp decrease of intercellular contacts, as well as cytoplasmic and nuclear degranulation (C). Bars = 2  $\mu$ m.

In HTR-8/SVneo cells at basal conditions we found the transcripts for Cx32, Cx37, Cx40, Cx43 and Cx45. After 1-h exposure of the samples to HF-EMF, the transcript levels for Cx40 and Cx43 increased significantly, while that for the other connexins remained unmodified. RF-EMF exposure was indeed shown to up- or down-regulate several genes associated with multiple cellular structures and function, such as the cytoskeleton, signal transduction pathway, metabolism, and connexons [36]. Since it was reported that an increase in Cx43 protects astrocytes against cell injury, and that Cx40 intensifies the resistance to calcium overload, oxidative stress, metabolic inhibition, tamoxiphene, and UV irradiation [37], the increased expression of Cx40 and Cx43 mRNA in response to irradiation could be interpreted as an attempt to enhance protein expression, in order to counteract injury. However, in our experimental model the up-regulation response to HF-EMF at the mRNA levels was not followed by variations in the related protein expression, as revealed by Western blot analysis of connexins. We suggest that the discrepancy observed after 1 h irradiation may be a consequence of rapid turnover due to intense protease activity, as reported for Cx43 in the adult rat heart [38]. The lack of the protein level increase following mRNA transcripts changes is however in agreement with previous data concerning different proteins and genes in EVT [9] and other cell systems [39].

Given the elevation of mRNA expression levels for Cx40 and Cx43, further experiments were carried out on these connexins. Although protein concentration were not modified, localization of both Cx40 and Cx43 revealed striking changes following HF-EMF exposure. At the plasma membrane level both proteins show

marked punctuate fluorescence in sham-exposed cells, while they exhibit a fluorescence diffusion in treated samples. Such a protein diffusion could account for the gap junction like structure decrease observed in our experiments at the ultrastructural level. Indeed, electron microscopy observations indicated that HF-EMF exposure induces a sharp decrease of cellular adhesion, gap junction-like structures being preserved only between tightly adherent cell islets. The Cx delocalization could be a consequence of HF-EMF influence on cell membrane fluidity. Changes in liposomal permeability were indeed observed in egg lecithin multilamellar vesicles after exposure to 900 MHz microwave radiation for 5 h [40]. However we cannot exclude that the ultrastructural changes induced by HF-EMF exposure derive from alterations other than Cx mRNA expression.

Since trophoblast Cx40 has been reported to participate in cell proliferation, while Cx43 is involved in syncytialization [13,14,31], it could be hypothesized that, once significantly increased, they could affect both processes up to the point of reaching clinical effects. In particular, Cx40 disappears when the proliferative cell phenotype changes to invasive, to be later re-expressed in the trophoblastic cell aggregates within the decidua [13,14,31], thus suggesting that its increment could impair invasive capacity. Extravillous trophoblast plays a fundamental role in modulating the maternal blood supply to the foetus by increasingly invading the uterine arteries during pregnancy. Therefore, a prolonged exposition to HF-EMF able to increase Cx that are known to regulate the above mentioned trophoblast function, could influence the mechanism by which oxygen and nutrients are delivered to the foetus, possibly leading either to positive effects, such as a better nutrition and

oxygenation, or to negative ones, such as foetal malformation and abortion.

Based on the above considerations it appears of outmost importance to further investigate both experimental and clinical implications of our results, by progressively increasing the time of trophoblast exposition to HF-EMF.

Searching for a possible influence of exposure on cellular physiology, we tested HTR-8/SVneo cell viability and a functional response. The cAMP signaling pathway was chosen since it plays important roles in these cells [30], and it is also related to the cell–cell communication events through gap junctions [17]. We found that 1-h treatment did not compromise viability, as revealed by the MTT test. Likewise, the adenylyl cyclase/cAMP signaling transduction pathway explored by assay of intracellular cAMP levels upon receptorial and non-receptorial activation of the enzyme, was not influenced by irradiation. Similarly, it has been reported that 6 h RF-EMF exposure of mouse embryonic stem cells transiently affects the transcript level of genes related to apoptosis and cell cycle control without any detectable change of cell physiology, thus suggesting a possible translational and post-translational compensatory mechanism [39].

In summary, our study indicates for the first time that 1 h exposure to GSM-217 Hz signals can selectively modify connexin mRNA expression pattern and protein localization in extravillous trophoblast derived HTR-8/SVneo cells. However, the up-regulation of Cx transcripts and protein delocalization induced by irradiation do not appear associated with detectable changes in the cell functional responses presently examined. More work providing further insights on possible effects of HF-EMF on cell–cell interactions in developing gestational tissues is advisable.

#### Conflict of interest statement

The authors declare that there are no conflicts of interest.

#### Acknowledgments

This work was supported by Grants from University of Ferrara (F.A.R. Biondi and Vesce) and Fondazione Cassa di Risparmio di Cento, Italy.

#### References

- [1] Kundi M, Mild K, Hardell L, Mattsson MO. Mobile telephones and cancer—a review of epidemiological evidence. *J Toxicol Environ Health B Crit Rev* 2004;7:351–84.
- [2] Valberg PA, van Deventer TE, Repacholi MH. Workgroup report: base stations and wireless networks-radiofrequency (RF) exposures and health consequences. *Environ Health Perspect* 2007;115:416–24.
- [3] Jensch RP. Behavioral teratologic studies using microwave radiation: is there an increased risk from exposure to cellular phones and microwave ovens? *Reprod Toxicol* 1997;11:601–11.
- [4] O'Connor ME. Intrauterine effects in animals exposed to radiofrequency and microwave fields. *Teratology* 1999;59:287–91.
- [5] Subbotina TI, Khadartsev AA, Yashin MA, Yashin AA. Effect of high-frequency low-intensity irradiation on reproductive function in C57Bl/6 and random bred mice. *Bull Exp Biol Med* 2004;138:554–5.
- [6] Ferreira AR, Knakiewicz T, Pasquali MA, Gelain DP, Dal-Pizzol F, Fernández CE, et al. Ultra high frequency-electromagnetic field irradiation during pregnancy leads to an increase in erythrocytes micronuclei incidence in rat offspring. *Life Sci* 2006;80:43–50.
- [7] Kwee S, Rasmak P, Velizarov S. Changes in cellular proteins due to environmental non-ionising radiation. *Electro Magnetobiol* 2001;20:141–52.
- [8] Valbonesi P, Franzellitti S, Piano A, Contin A, Biondi C, Fabbri E. Evaluation of HSP70 expression and DNA damage in a human trophoblast cell line exposed to 1.8 GHz amplitude-modulated radiofrequency fields. *Radiat Res* 2008;169:270–9.
- [9] Franzellitti S, Valbonesi P, Contin A, Biondi C, Fabbri E. HSP70 expression in human trophoblast cells exposed to different 1.8 GHz mobile phone signals. *Radiat Res* 2008;170:488–97.
- [10] Lunghi L, Ferretti ME, Medici S, Biondi C, Vesce F. Control of human trophoblast function. *Reprod Biol Endocrinol* 2007;5:6–19 [Review].
- [11] Chakraborty C, Gleeson LM, McKinnon T, Lala PK. Regulation of human trophoblast migration and invasiveness. *Can J Physiol Pharmacol* 2002;80:116–24 [Review].
- [12] Cronier L, Bastide B, Defamie N, Niger C, Pointis G, Gasc JM, et al. Involvement of gap junctional communication and connexin expression in trophoblast differentiation of the human placenta. *Histol Histopathol* 2001;16:285–95 [Review].
- [13] Cronier L, Defamie N, Dupays L, Theveniau-Ruissy M, Goffin F, Pointis G, et al. Connexin expression and gap junctional intercellular communication in human first-trimester trophoblast. *Mol Hum Reprod* 2002;8:1005–13.
- [14] Nishimura T, Dunk C, Lu Y, Feng X, Gellhaus A, Winterhager E, et al. Gap junctions are required for trophoblast proliferation in early human placental development. *Placenta* 2004;25:595–607.
- [15] Malassiné A, Cronier L. Involvement of gap junctions in placental functions and development. *Biochim Biophys Acta* 2005;1719:117–24 [Review].
- [16] Wei CJ, Xu X, Lo CW. Connexins and cell signaling in the development and disease. *Annu Rev Cell Dev Biol* 2004;20:811–38 [Review].
- [17] Willecke K, Eiberger J, Degen J, Eckardt D, Romualdi A, Guldenagel M, et al. Structural and functional diversity of connexins genes in the mouse and human genome. *Biol Chem* 2002;383:725–37 [Review].
- [18] Oyamada M, Oyamada Y, Takamatsu T. Regulation of connexin expression. *Biochim Biophys Acta* 2005;1719:6–23 [Review].
- [19] Jeong SH, Habeebu SS, Klaassen CD. Cadmium decreases gap junctional intercellular communication in mouse liver. *Toxicol Sci* 2000;57:156–66.
- [20] Azzam EI, de Toledo SM, Little JB. Expression of Connexin 43 is highly sensitive to ionizing radiation and other environmental stresses. *Cancer Res* 2003;63:7128–35.
- [21] Irving JA, Lysiak JJ, Graham CH, Hearn S, Han VK, Lala PK. Characteristics of trophoblast cells migrating from first-trimester chorionic villus explants and propagated in culture. *Placenta* 1995;16:413–33.
- [22] Spencer WE, Christensen MJ. Multiplex relative RT-PCR method for verification of differential gene expression. *BioTechniques* 1999;27:1044–52.
- [23] Czyn J, Guan K, Zeng Q, Nikolova T, Meister A, Schönborn F, et al. High frequency electromagnetic fields (GSM signals) affect gene expression levels in tumor suppressor p53-deficient embryonic stem cells. *Bioelectromagnetics* 2004;25:296–307.
- [24] Schönborn F, Pokovic K, Wobus AM, Kuster N. Design, optimization, realization, and analysis of an *in vitro* system for the exposure of embryonic stem cells at 1.71 GHz. *Bioelectromagnetics* 2000;21:372–84.
- [25] Mosman T. Rapid colorimetric assay for cellular growth and survival: application to proliferation and cytotoxicity assays. *J Immunol Methods* 1983;65:55–63.
- [26] Brown BL, Ekins RP, Albano JD. Saturation assay for cyclic AMP using endogenous binding protein. *Adv Cyclic Nucleotides Res* 1972;2:25–40.
- [27] Laemmli UK. Cleavage of structural proteins during the assembly of the heat of bacteriophage T4. *Nature* 1970;227:680–5.
- [28] Lowry OH, Rosebrough NJ, Farr AL, Randall RJ. Protein measurement with the Folin phenol reagent. *J Biol Chem* 1951;193:265–75.
- [29] Piano A, Valbonesi P, Fabbri E. Expression of cytoprotective proteins, heat shock protein 70 and metallothioneins, in tissues of *Ostrea edulis* exposed to heat and heavy metals. *Cell Stress Chaperones* 2004;9:134–42.
- [30] Biondi C, Ferretti ME, Pavan B, Lunghi L, Gravina B, Nicoloso MS, et al. Prostaglandin E<sub>2</sub> inhibits proliferation and migration of HTR-8/SVneo cells, a human trophoblast-derived cell line. *Placenta* 2006;27:592–601.
- [31] Winterhager E, von Ostau C, Gerke M, Grümmer R, Traub O, Kaufmann P. Connexin expression patterns in human trophoblast cells during placental development. *Placenta* 1999;20:627–38.
- [32] Al-Lamki RS, Skepper JN, Burton GJ. Are human placental bed giant cells merely aggregates of small mononuclear trophoblast cells? An ultrastructural and immunocytochemical study. *Hum Reprod* 1999;24:496–504.
- [33] Kibschull M, Gellhaus A, Winterhager E. Analogous and unique functions of connexins in mouse and human placental development. *Placenta* 2008;29(10):848–54.
- [34] Khoo NKS, Zhang Y, Bechberger JF, Bond SL, Hum K, Lala PK. SV40 Tag transformation of the normal invasive trophoblast results in a premalignant phenotype. II. Changes in gap junctional intercellular communication. *Int J Cancer* 1998;77:440–8.
- [35] Schuderer J, Samaras T, Oesch W, Spät D, Kuster N. High peak SAR exposure unit with tight exposure and environmental control for *in vitro* experiments at 1800 MHz. *IEEE Transac Microw Theory Tech* 2004;52:2057–66.
- [36] Zhao R, Zhang S, Xu Z, Ju L, Lu D, Yao G. Studying gene expression profile of rat neuron exposed to 1800 MHz radiofrequency electromagnetic fields with cDNA microarray. *Toxicology* 2007;235:167–75.
- [37] Lin JH-C, Yang J, Liu S, Takano T, Wang X, Gao Q, et al. Connexin mediates gap junction-independent resistance to cellular injury. *J Neurosci* 2003;23:430–41.
- [38] Beardslee MA, Laing JG, Beyer EC, Saffitz JE. Rapid turnover of connexin 43 in the adult rat heart. *Circ Res* 1998;83:629–35.
- [39] Nikolova T, Czyn Y, Rolletschek A, Blyszczuk P, Fuchs J, Jovtchev G, et al. Electromagnetic fields affect transcript levels of apoptosis-related genes in embryonic stem cell-derived neural progenitor cells. *FASEB J* 2005;19:1686–8.
- [40] Gaber MH, Abd El Halin N, Khalil WA. Effect of microwave radiation on the biophysical properties of liposomes. *Bioelectromagnetics* 2005;26:194–200.